Making hard x-ray micro-focus beam and imaging microscopy with Fresnel zone plate optics

-SPring-8 summer school text-

Sept. 2008

Revised June 2009,

Revised October 2009 (Imaging microscop)

Yoshio Suzuki, JASRI/SPring-8

Contents

1. What is Fresnel zone plate for hard x-rays?

1.1. Introduction - a simple and intuitional explanation of Fresnel zone plate (FZP) -

It is difficult to use refractive optics in the hard x-ray regions, while the refractive lens is most popular optics for visible light. This is because the index for refraction in the x-ray region is very near to the index for refraction of vacuum. The discrepancy from unity is only 10^{-5}-10^{-6} for any materials. Therefore it is very difficult to deflect the x-ray beam by refraction at the interface of optical media, and any optical devices that are used in visible light optics, lens or prism, cannot be used for x-rays, as it is. Although, some refractive lenses or prisms are developed in the hard x-ray region, they are still rare case. At present, the Fresnel zone plate (FZP) is a widely used and practical optics device in the x-ray regions, the x-ray energy around 10 keV or higher energy regions. The micro-focus beam size of about 30 nm is already achieved with the FZP optics in the hard x-ray region.

The Fresnel zone plate is a concentric transmission grating with radially decreasing grating period, as schematically shown in Fig. 1.1, coarse grating period at central part, and finer pitch at the outer (marginal) area. An optical micrograph of FZP is shown in Fig. 1.2. This is a real Fresnel zone plate used as micro-focusing optics or image forming optics at the SPring-8 beamlines.

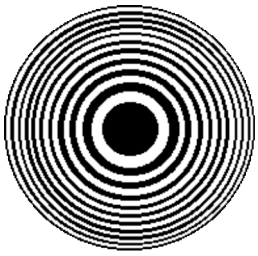

Fig.1.1. Schematic drawing of FZP structure. The radius of n-th ring is defined by $r_n = \sqrt{(n\lambda f)}$. λ is x-ray wavelength and f is focal length.

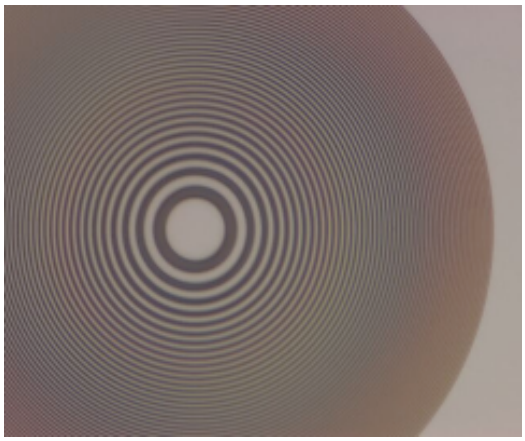

Fig. 1.2. An optical micrograph of FZP used at the SPring-8 imaging beamlines as microfocus lens and/or

microscope objective lens. The diameter of FZP is 100 μm and the outermost zone pitch (period) is 0.5 μm. The focal length of the FZP is designed to be 248 mm for 1.0 Å (12.4 keV) x-rays. The zone structure is made of 1 μm-thick tantalum deposited on a 2 μm-thick silicon nitride membrane. This FZP will be used in our experimental course.

In order to understand the FZP optics intuitionally, it is useful to start from two-slit optics, so called Young's double-slit. The two-slit is a most simple and basic tool in wave optics. As shown in Fig. 1.3, when a pair of slit is placed with a distance of d, intensity distribution on a screen far from slit has periodic structure. When the observation angle θ satisfy an equation, $n\lambda = d \sin\theta$, the intensity is maximum, and minimum is observed at $(n + 1/2)\lambda = d \sin\theta$. Here, n is an integer number called order of diffraction. If the incident radiation is perfectly coherent and the slit width is negligibly narrow, the observed intensity distribution must be sinusoidal! But the perfect coherence is not realistic in general experimental condition. Therefore, the actual interference pattern becomes weak far from optical axis, as shown in Fig. 1.3.

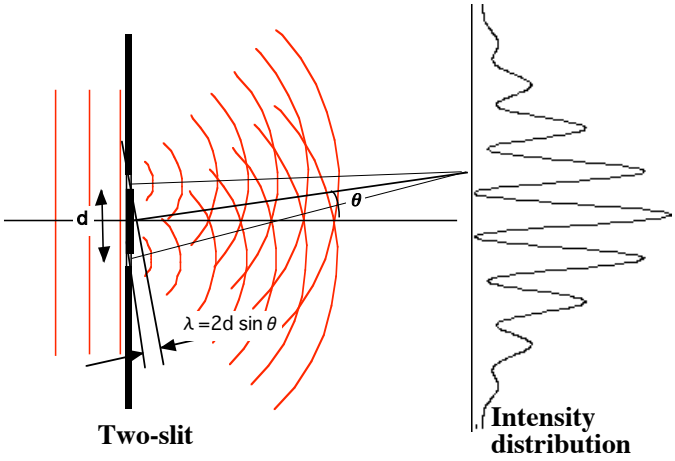

Fig. 1.3. Schematic diagram of Young's two-slit experiment and its interference pattern. Gaussian type spatial coherence is assumed for numerical calculation of interference pattern.

Next, let us consider diffraction by grating: a periodic slit array. As shown in Fig. 1.4, the beam deflection angle at a grating with a period of d is described as $\sin\theta = n\lambda/d$, where $n = 0, \pm1, \pm2, \pm3,,,,,$. The integer n is also called order of diffraction. The $n = 0$ is undiffracted beam.

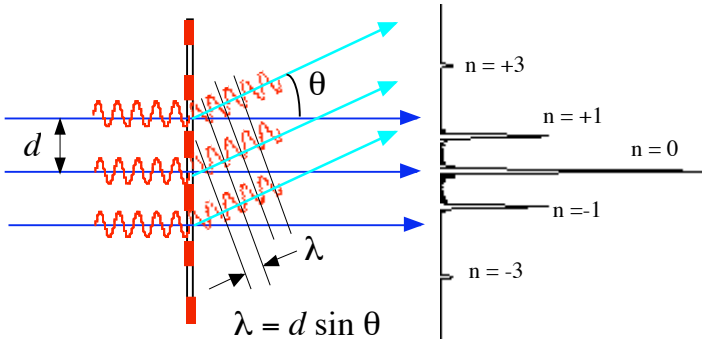

Fig. 1.4. Linear grating and diffraction pattern by the grating. The intensity distribution (diffraction pattern of grating) is given by the Laue function as $sin^2(\pi N d sin\theta)/sin^2(\pi d sin\theta)$, where N is number of grating period. Even order diffractions, n = 2, 4, 6 ,,, are not allowed for 1:1 ratio of obstacle and transparent area, and higher order diffractions are weaker than the fundamental diffraction.

When the grating period is changed as $d = \lambda/sin\theta$, as shown in Fig. 1.4, all the diffracted rays are focused at a point, where θ is determined by $tan\theta = r/f$, and the r is radius of circular grating, and f is a specific distance from zone plate.

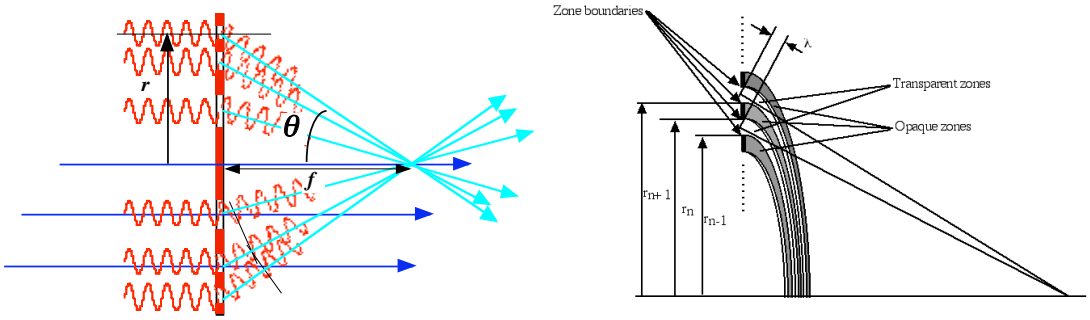

Fig. 1.5. Diffraction at Fresnel zone plate (schematic diagram), and focus of x-ray beam.

The specific length f is called focal length. Assuming $\theta << 1$, this condition is usually satisfied in the hard x-ray region, diffraction condition, $d\theta \sim \lambda$, for n-th ring can be written as

$$(r_{n+1} - r_{n-1})\, r_n / f \sim \lambda,$$

where, $\theta \sim r_n /f$, and $d \sim (r_{n+1} - r_{n-1})$. Then, regarding the above equation as a differential equation of

$$2\partial r(n)/\partial n = \lambda f / r(n).$$

By solving the above equation, we can get an equation for Fresnel zone plate structure as

$$r_n^2 \sim n\lambda f + \text{Const.},$$

generally Const. = 0, and $r_n = \sqrt{(n\lambda f)}$.

This is only an approximation, because the above discussion is valid only for large n and small diffraction angle. However, this intuitional explanation is very useful for understanding the geometrical meaning of FZP optics.

As is understandable from these considerations, there are positive and negative orders of diffraction. Thus, the zone plate acts as a convex lens for visible light, and it simultaneously works as a concave lens with negative order diffraction. The 0^{th} order and higher order diffractions usually exist. Therefore, a kind of spatial filtering is needed in FZP optics to work as an optical lens. A typical method of selecting a required order of diffraction is putting a small diaphragm near the focal point. When the diameter of aperture is sufficiently smaller than the FZP diameter, the undesired order of diffractions including direct beam are suppressed enough. If the suppression is not sufficient, an additional beam stop disc may be used for diffraction order selection as shown in the figure. This beam stop disc is usually added in fabrication process of FZP, and it is called center stop, or center obstacle. The aperture near the focus is called order-selecting-aperture (OSA), or sometimes order-sorting-aperture.

When a central beam stop of diameter r_0 is used, the zone plate structure can be modified as

$$r_n^2 \sim n\lambda f + r_0^2.$$

Above formula is widely used for general FZP that is fabricated together with central beam stop disc. Then, the first zone stars from r_0, and the inner radius of second zone radius is $r_1 = \sqrt{(\lambda f + r_0^2)}$.

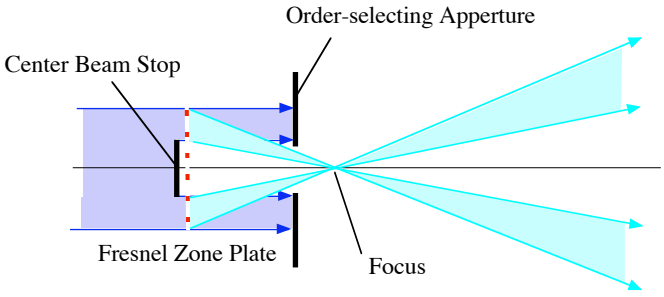

Fig. 1.6. Diffraction-order-selection in FZP microbeam optics.

1. 2. More precise treatment of FZP optics

The exact equation of FZP structure is obtained by optical path difference and expansion of Fermat's principle. The Fermat's principle is that an actual optical path between any two points should be shorter than any other paths that connect the two points. By considering the finite wavelength, the *n*-th zone boundary of a Fresnel zone plate that focuses the spherical wave emitted from point A to the point B is expressed by the following equation,

$$(R_a + R_b) = n\lambda/2 + (a + b),$$

as shown in Fig. 1.7, and

$$(a^2 + r_n^2)^{1/2} + (b^2 + r_n^2)^{1/2} - (a + b) = n\lambda/2, \qquad (1.1)$$

where a is a distance from point A to the FZP, b is a distance between B and FZP, and r_n is n-th boundary of zone structure, and n is integer. This formula is a basic and exact equation of Fresnel zone structure. Expanding with r_n and neglecting higher order terms, the equation (1.1) is rewritten as

$$a + r_n^2/2a + b + r_n^2/2b - (a + b) = n\lambda/2. \qquad (1.2)$$

Then,

$$r_n^2/a + r_n^2/b = n\lambda. \qquad (1.3)$$

Again, by defining $1/a + 1/b = 1/f$, the equation (1.3) is rewritten as

$$r_n^2 = n\lambda f. \qquad (1.4)$$

The equation, $1/a + 1/b = 1/f$, is well-known Newton's lens equation. Thus, an FZP whose zone boundary is defined by the above equation works as a lens with a focal length of f.

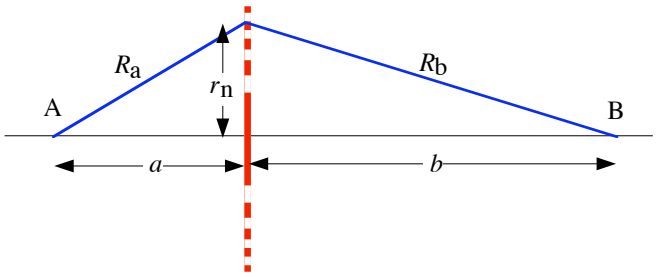

Fig. 1.7. Optical path description of Fresnel zone plate

1.3. Diffraction efficiency of FZP

The diffraction efficiency is an important characteristic of diffraction-based optics, because the intensity of focused beam is mainly determined by the diffraction efficiency, and the diffractive optics such as FZP or grating can gather only a portion of incident radiation. The diffraction efficiency of FZP is equivalent to the linear grating. Therefore, we can calculate it by solving one-dimensional Kirchhoff's integral for single period of gating. For instance, first order diffraction of opaque and transparent zone structure with 1:1 zone ratio, the intensity of diffracted beam is given by

$$I = |E|^2, \text{ and } E = \int C * \exp(ik\, x \sin\theta)\, dx,$$

Here, the integral is taken for one cycle, d, of grating, and $2\pi/k = \lambda = d \sin\theta$. The constant C = 1 for transparent area, and C = 0 for opaque zone. Then, for the first-order diffraction,

$$E = \int \exp(2\pi i/d)\, dx = 2$$

By normalizing with the incident beam intensity of $(2\pi)^2$, $I = 4/(2\pi)^2$ ($=1/\pi^2$ ~ only 10% for 1st-order diffraction). The general form for n-th order diffraction can be easily calculated by the similar manner. It is known that the n-th order diffraction efficiency for transparent and opaque zone, i.e., black and white zone, with even zone width (1:1 zone ratio) is $1/(n\pi)^2$, where $n = \pm1, \pm3, \pm5,,,,$. The even order diffraction does not exit for the grating with 1:1 groove width.

More efficient grating is realized by the phase-modulated structure that is the utilization of phase shift through the zone, instead of stopping the beam with opaque zone. The maximum diffraction efficiency is attained at a phase shift of half wavelength (phase shift of π). The efficiency of n-th order diffraction for ideal phase grating of 1:1 zone ratio is $4/(n\pi)^2$ ($n = \pm1, \pm3, \pm5,,,,$). So, the first order diffraction has an efficiency of about 40% in the case of ideal phase-modulated zone plate. However, in

the x-ray region, pure phase material without absorption dose not exist. All the optical media is complex of phase and absorption effect.

More efficient FZP can be made by using so-called kinoform structure, that is recently introduced in hard x-ray regions. Optimized kinoform FZP can give nearly 100% efficiency, if the absorption loss can be ignored. Real diffraction efficiency is lower than 100%, but the diffraction efficiency of higher than 50% is already achieved in the hard x-ray region with quasi-kinoform structure.

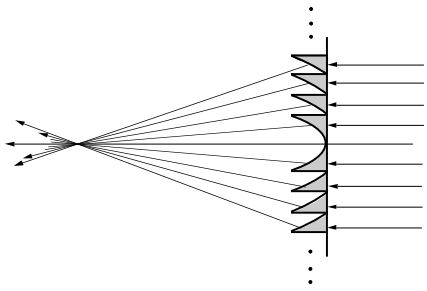

Fig. 1.8. Schematic diagram of kinoform zone plate.

1.4. Fabrication of zone plates:

Most of zone plate for x-ray microscope is fabricated by using a state-of-art technology developed in semiconductor technology, i.e., electron-beam lithography technique. Recent ULSI technology makes it possible to fabricate sub-100 nm microstructure on a silicon tip. This is also a key technology in x-ray microscopy. Schematic drawing of cross sectional structure is shown in Fig. 1.9. The zone plate pattern is drawn by electron-beam to the resist on thin membrane on silicon wafer. The thin membrane is usually a few μm-thick silicon nitride or silicon carbide. The pattern transfer from photo-resist to zone material is done by reactive dry-etching process or wet electroplating process (usually, dry-etching is used for tantalum, and electroplating is employed for gold pattern). Finally, the silicon wafer of pattering area is removed by chemical etching process, as shown in the figure.

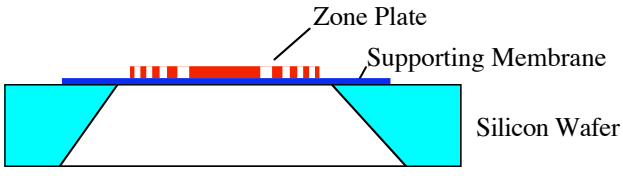

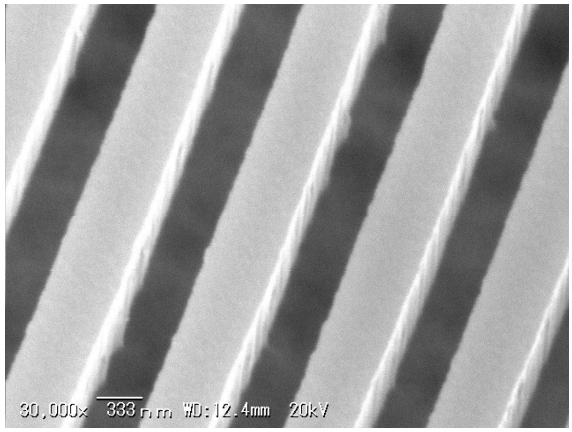

Fig. 1.9. Structure of Fresnel zone plate. Cross-sectional view and SEM micrograph.

The difficulty on fabrication of x-ray zone plate is high aspect ratio (zone-height/zone-width) of zone structure at the marginal zone area. In the hard x-ray region, the phase shift is much greater than the absorption contrast even for the high-Z elements. Therefore, most of the x-ray FZPs is designed as a phase-modulation zone plate. Assuming a free electron approximation, the real part of index for refraction, n, for x-rays is written as

$$\mathrm{Re}(n) = 1 - \delta,$$

$$\delta = 1.35 \times 10^{-6} \rho(\mathrm{g/cm^3}) \lambda (\mathrm{Å})^2,$$

where ρ is density of material, and Z/A = 1/2 is also assumed (Z: atomic number, A: atomic weight). The optimum thickness of zone plate, t, is equivalent to the optical path difference of $\lambda/2$, that is calculated by $t\delta = \lambda/2$. Then, high dens material is preferable for zone plate. Considering the manufacturing process of microstructure, gold or tantalum is usually chosen as a zone material for hard x-ray FZP. The optimized thickness and δ for tantalum zone plate, for instance, is 2.9 μm and 1.71×10^{-5} at an x-ray wavelength of 1.0 Å, respectively. Then, the aspect ratio should be 29 for the FZP having 100 nm-zone-width. The required aspect ratio is still challenging even in the present nano-fabrication technology. The resolution limit of FZP (width of outermost zone) is being improved year by year, and the finest zone structure of about 20 nm is possible at present. However, the thickness of these high resolution FZPs is far from ideal value for hard x-rays.

2. Making microfocus beam with Fresnel zone plate

2.1. How is the limit of focused beam size? Diffraction limit and geometrical limit of resolution

The microbeam optics is to demagnify the light source image with an optical lens or mirror. Therefore, the generated microbeam size is firstly determined by the magnification ratio and source size, i.e. geometrical definition. However, there is another significant limitation on beam focusing, that is limitation due to diffraction of wavefield.

Ultimate spatial resolution (focused beam size limit) of imaging optics is determined by the diffraction of light. The diffraction-limited resolution is deduced from the uncertainty principle in quantum mechanics. If a photon is squeezed within a small space of $<\Delta x>$, the momentum uncertainty of photon, $<\Delta p>$, is given by following formula,

$$<\Delta x><\Delta p> \geq h/2\pi,$$

where h is the Plank constant. Consequently, larger spread of momentum is required to focus (localize) a photon in a smaller area. This is a fundamental limitation of microfocus beam size. The momentum of photon is given by the formula, $p = h/\lambda$, and the uncertainty of momentum is related to the angular spread of momentum. As shown in the figure, when a parallel incident beam is focused by a lens, the angular spread of focused-photon's momentum becomes $(h/\lambda)sin\theta$, and momentum uncertainty becomes $\Delta p = \pm (h/\lambda)sin\theta$. Then the limit of focused beam size, Δx, can be written as

$$\Delta x \geq 2h/(2\pi\Delta p) \sim \lambda/(\pi sin\theta),$$

The term, $sin\theta$ is known as numerical aperture (NA) of lens. The *F-number* defined by $F = 1/NA$ is usually used in optical instruments instead of NA. In the hard x-ray region, the $NA << 1$, and $sin\theta$ is approximately equal to r_N/f, where the r_N is radius of outermost zone.

This discussion is one-dimensional condition, and we cannot get an exact form of intensity distribution. The lens optics, including FZP optics, is an axis-symmetric system. For the axisymmetric optical systems, the formula of the resolution limit is slightly deformed as

$$\Delta x = 0.61\ \lambda/NA,$$

This definition is well known Rayleigh's criterion for spatial resolution of microscope with an objective

lens of circular aperture. This formula was obtained by a classical diffraction theory for electromagnetic wave, far before the birth of quantum physics, but essentially the same as that derived from quantum mechanics. This relation comes from a definition of quantum photon momentum, $p = h/\lambda$.

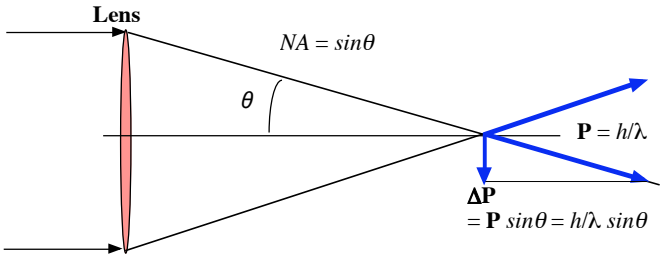

Fig. 2.1. Numerical aperture of objective lens.

The diffraction limit can also be explained by a simple diffraction theory for single slit, as described below. When a parallel and monochromatic beam is incident on a slit with an opening of w (one dimensional case), the propagating wave through the slit is not a parallel wave anymore.
Using the Kirchhoff-Huygens' principle, the electromagnetic wave field is given by an integral formula of

$$E(\theta) = \int \exp(ik\, x \sin\theta)\, dx$$

Here, k is a wave number defined by $k = 2\pi/\lambda$. Taking a integral over the slit opening, the amplitude of electromagnetic wave far from the slit is given by the following function.

$$E = \sin(kw/2 \sin\theta) / (kw/2 \sin\theta).$$

The function $(sinX)/X$ is the *sinc function* which frequently appears in the diffraction theory. The beam intensity far from slit takes maxima on the optical axis ($\theta = 0$), and first zero (local minimum) at

$$(kw/2 \sin\theta) = \pi,$$
$$\text{or} \quad \lambda = w \sin\theta \sim w\theta,$$

because w is usually much greater than wavelength in the hard x-ray region. Thus, the angular spread (blurring) of the propagating wave is broadened by passing a slit. It is equivalent that a finite angular convergence of incident beam is required to focus the beam within a limited area. Saying differently, a finite divergence of outcoming wave is always accompanied by focusing a photon beam. This result of the diffraction theory of electromagnetic wave is essentially the same as the uncertainty principle in the

quantum physics.

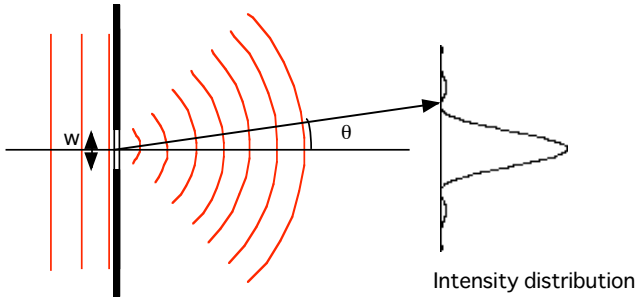

Fig. 2.2. Diffraction by a single slit. Radiation through the slit is broadened by propagating in a free space.

It is also apparent from the diffraction by a grating that the $sin\theta$ is equal to λ/d, where d is the outermost zone period of FZP. Then, for the circular grating (FZP without center stop), the diffraction-limited resolution is defined as

$$\Delta x = 0.61d.$$

A formula of $\Delta x = 1.22\ dr_N$ is frequently used instead of above equation, where dr_N is a half pitch of the outermost zone period (or width of outermost zone). Then, the ultimate limit of the focused beam size is nearly equal to the width of outermost Fresnel's zone of the objective FZP. This relation can also be derived from the Fresnel zone plate equation and the formula of diffraction-limited resolution.

However, the actual focus is generally limited by the quality of incident beam. We have implicitly assumed a parallel beam for explaining how the FZP works as a beam focusing element. But, in any light sources, the emitted radiation is neither a perfect plane wave, nor a perfect spherical-wave. The radiation is emitted from a finite source area, and is emitted in random direction, a chaotic source! In this case, the beam focusing should be considered as generation of a demagnified image of the light source. This limitation of focused beam size is known as the geometrical optics limit. This operation of microfocusing optics is similar to that of telescope optics. As shown in Fig. 2.3, the light source image is formed at focus by a magnification factor of b/a according to the Newton's equation. Then the focused image size, S_b, is given as

$$S_b = S_a\, b/a,$$

where S_a is source dimension, a is source to lens distance, and b is lens to focus distance. Usually $a >> b$,

then $b \sim f$. A long distance from source point or a small source size is necessary to achieve small (micro) focus beam. The factor S_a/a is sometimes called angular size of light source. In most synchrotron radiation facilities, the angular size is not small enough to generate microfocus beam, and the distance is limited by beamline length. So, we need to makeup a virtual source by putting a small pinhole (or slit) at the upstream section of the beamline. The slits equipped at beamline, front-end slit or transport-channel slit, are usually used as the virtual source for micro-focusing experiment. It is also important that there are no disturbances of wave front by the optical elements in the beamline. The monochromator crystals, mirrors, and vacuum windows usually tend to give serous deformation of the x-ray beam direction and the wavefront shape.

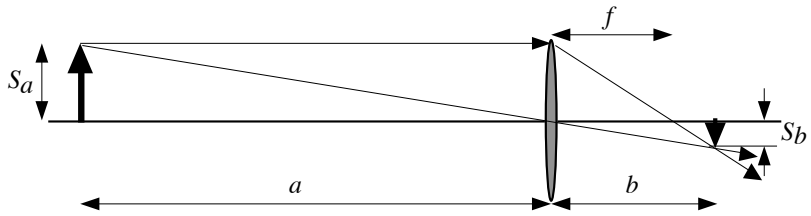

Fig. 2.3. Geometrical description of beam focusing optics

2.2. Depth of focus and chromatic aberrations

If the wavelength is slightly different from designed value, the focus slightly moves on the optical axis. That means different wavelength x-rays are focused at a different position. The focal length f varies inversely as the wavelength of x-rays. These phenomena are called chromatic aberrations. Therefore, monochromatic x-ray beam is required for FZP microbeams. Saying differently, the FZP microbeam optics can be used as a monochromator or spectrometer.

Geometrical beam size at a distance of Δf from the exact focus can be calculated to be $2NA\,\Delta f$, as shown in Fig. 2.4. This value should be smaller than the diffraction-limited resolution in order to achieve the full-performance of FZP optics. Then the condition can be written as

$$0.61\,\lambda/NA \geq 2NA\,\Delta f,$$

or using the FZP equation, we can get a simple and useful formula, as

$$0.61/(2N) \geq \Delta f/f.$$

Here, N is number of Fresnel zone.

The chromatic aberration is also estimated by similar manner, because $\Delta f/f = -\Delta\lambda/\lambda$ from the FZP equation. So, the chromatic aberration is characterized by the number of Fresnel zone, N.

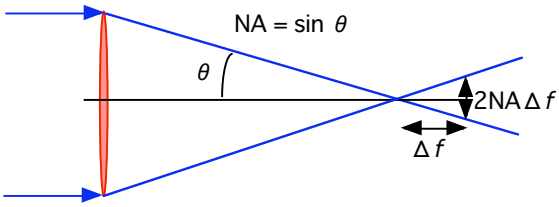

Fig. 2.4. Depth of focus

2.3. Preservation of emittance and brilliance

An important law in beam-focusing optics is described in this section. An emittance preservation rule. As shown in Fig. 2.5, when a magnified (or demagnified) image of light source is formed by an optical element, there is a relation between the image dimension, S_a, S_b, and angular spread, θ_a, θ_b as

$$S_a \, \theta_a = S_b \, \theta_b \, .$$

The product of beam dimension and angular spread, $S\theta$, is called the beam emittance, and the above formula represents the emittance preservation rule. This emittance preservation is deduced by the geometrical optics. The efficiency of optical system is not 100%, even if a perfect lens (without any aberrations) is used. This is because the focus beam size is limited by the diffraction. Therefore, the equation should be rewritten as

$$S_a \, \theta_a \leq S_b \, \theta_b \, ,$$ for general optics.

If the absorption loss at optical system is ignorable, the flux of focused beam, I_b, is equal to the flux of the incident radiation, I_a, as

$$I_b \leq I_a$$

and $I_b = I_a$ for ideal case.

Then, flux, I, divided by the source dimension, S, and the angular divergence, θ, is constant as

$I_b, / (S_b\ \theta_b) = I_a / (S_a\ \theta_a)$, for the ideal optics.

This relation is called brilliance preservation rule, and the flux density limit of focused beam is determined by this equation. The flux density of the focused beam is generally higher than that of the unfocused beam, where the unfocused beam is a microbeam generated simple by putting a micro-pinhole in front of sample. Although, the beam intensity seems to increase by focusing, there is no real gain of beam brilliance. The brilliance is always preserved in any ideal optical systems, and the actual brilliance always decreases by passing through the optical element, because the throughput, reflectivity of mirror or diffraction efficiency of gating and FZP, is always less than 100%. Remember that any optical systems decrease the brilliance, and increase the emittance. The highest brilliance is obtained only at the initial source point! This is an important principle of beam focusing optics.

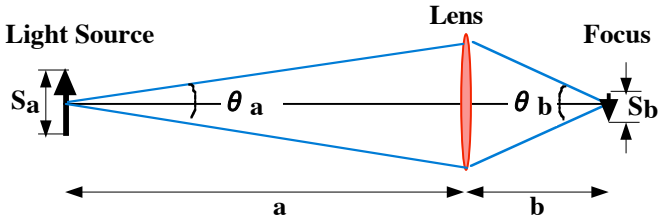

Fig. 2.5. Schematic diagram of emittance preservation rule

2.4. General description of focusing optics

In the above sections, we focused only on the Fresnel zone plate optics for x-ray focusing. Even in the x-ray regions, various types of beam focusing, or imaging, devices are developed, such as total reflection mirrors, multi-layer optics, Bragg Fresnel lenses, multi-layer Laue lenses, etc. These optical elements are, however, able to be described by a simple form of extended Fermat's principle.

His (Fermat's) idea is this: That out of all possible paths that it might take to get from one point to another, light takes the path which requires the shortest time (the least possible time),

and an application of the Fermat's principle is that,

We want to bring all the light back to what we call a focus. How? If the light always takes the path of least time, then certainly it should not want to go over all these other paths. The only way that the light can be perfectly satisfied to take several adjacent paths is to make those times exactly equal! (Lectures on Physics by R. Feynman) Then, with wavelength λ of light, all the different paths with optical path difference of $n\lambda$ are also allowed as shown in Fig. 2.6.

The P_n represents ellipse with foci F_1 and F_2. The ellipse is an ensemble of points that have the property that the sum of the distances from two points is a constant. A plane ellipse is used for one-

dimensional focusing, and ellipse of rotation (ellipsoid) for 2D focusing. A single ellipse or ellipsoid , for example, represents total-reflection-mirror optics. All kinds of beam focusing optical system can be understood using the formula of

$$P_n = P_0 + n\lambda,$$

where n is integer, and λ is wavelength. P_0 is an ellipse with foci F_1 and F_2. Now, the Fresnel zone plate can be regarded as an approximation of ellipsoids that consists of only the pints on a plane S_1 that is normal to the optical axis. The S_2 and S_3 represent Bragg Fresnel lens. The S_2 also represents an approximation of self-focusing grating. The total reflection mirror system is represented by a shell of ellipse or ellipsoid. The multi-layer Laue lenses and multi-layer mirrors can also be understood as a three-dimensional structure that consists of ensemble of ellipses or ellipsoids. Therefore, all the optical devices utilizing reflection or diffraction, except for refractive lens, are only an approximation of the nesting ellipse shown in the figure. The ellipse and ellipsoid should be replaced by parabola and paraboloid for parallel beam or a point source at infinite distance, and hyperbola and hyperboloid for convergent beams.

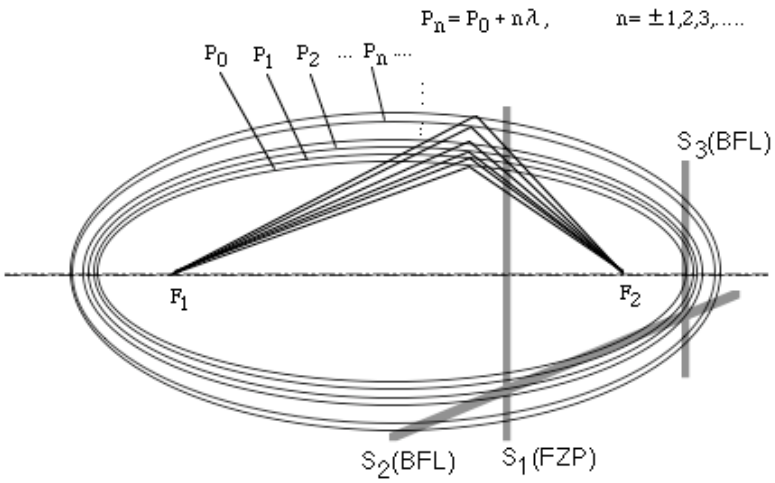

Fig. 2.6. General description of focusing optics.

3. Application of FZP optics to imaging microscopy and microtomography

3.1. X-ray imaging microscopy

Limitation of spatial resolution for conventional imaging system such as projection imaging is usually determined by spatial resolution of imaging detector. The development of high-resolution detectors, spatial resolution of μm – nm, is very difficult task in the hard x-ray region. Although, high-resolution photo-resists for x-ray lithography have spatial resolution better than 100 nm, they cannot be applied to general use, because linearity of the photo-resist is insufficient and real time imaging processing is usually required in microscopy.

There is another limitation of projection imaging. Geometrical optics approximation is assumed in projection imaging and contact microscopy. This assumption is generally valid for the medical imaging instruments because of short wavelength (~0.2 Å) and low spatial resolution (~mm). However, even in hard x-ray region, diffraction at the object cannot be ignored for high-resolution imaging. The spatial resolution of measured image is deteriorated by the diffraction at the specimen. Thai is caused by diffraction at specimen. Image blurring due to Fresnel diffraction of x-rays cannot be neglected in the high-resolution imaging. The amount of blur for Fresnel diffraction is approximately $(\lambda L)^{1/2}$, where λ is x-ray wavelength. The L represents the distance between sample and detector in the case of contact microscopy, and it corresponds to the distance from source point to sample in the case of projection imaging with a spherical wave from small point source, i.e. cone beam projection imaging with high magnification. When $\lambda = 1$ Å and $L = 1$ cm, the image blur becomes 1 μm. Therefore, high-resolution imaging is difficult, if simple projection imaging scheme is used. Microscopy in combination with the holographic image reconstruction is provably only an exception.

The use of x-ray imaging optics is one of the best ways to resolve this problem. By using the x-ray high-magnification imaging-objective optics, the effects of Fresnel diffraction and limitation of imaging detector can be solved. Then, the ultimate limit of spatial resolution is thickness of specimen. Image blurring caused by the beam deflection inside of the object is now expressed as $(\lambda L)^{1/2}$, where the L now represents the thickness of specimen. This limitation is related to the depth of focus of objective lens. The zone plate optics is widely used in the hard x-ray microscopy, and spatial resolution of better than 100 nm is already achieved in the hard x-ray region with the FZP objective. The imaging property of FZP objective is very suitable for hard x-ray microscopy, because off-axis aberrations of FZP optics are usually negligible in hard x-ray region..

3.2. Order selection by spatial filter and illuminating optics for FZP objective

As described in the previous section, the FZP cannot be used as conventional refractive lens because of existence of undesirable diffractions. A simple way of diffraction order selection is shown in Fig. 3.1. The object and objective is illuminated by a planar wave with a cross-section limited by a diaphragm, and only a half of FZP objective is illuminated. Then, positive order diffraction and negative order one is well separated at the image plane, and the direct beam appears at the boundary between the positive diffraction and negative diffraction. The optical system shown in Fig. 3.1 is called off-axis illumination. The configuration shown in the figure cannot separate higher order diffraction. Additional spatial filters are needed for perfect order-selection. However, higher order diffraction has much low efficiency and large magnification at the image plane. Therefore, higher order diffraction is usually ignorable. The serious problem of off-axial illumination is non-uniformity of imaging property, i.e. strong edge-enhancement in the marginal region of image field. Therefore, spatial filtering by combining with condenser optics is commonly used in imaging microscopy with FZP objective. There are typically two types of illumination optics for imaging microscopy, critical illumination and Köhler's illumination.

The schematic diagrams of critical illumination and Köhler illumination are shown in Fig. 3.2a and 3.2b. The critical illumination, however, is not suitable for synchrotron radiation light source, because the synchrotron radiation light source has small source dimension and narrow divergent angle. In the critical illumination, a demagnified image of the source is formed at the object plane by the condenser lens. Then, the typical field of view becomes only a few μm in the general synchrotron radiation beamlines. On the other hand, the condenser optics for the Köhler's illumination does not generate the demagnified image. A constant angle deflection is done by the condenser lens optics, and the deflected beams are merged together in the field of view of objective lens. The Köhler illumination results in a hollow cone beam behind the objective, as shown in the figure. This condenser optics is realized by using a constant period zone plate with a center beam stop (not a Fresnel zone plate) or by using a rotating double-mirror mechanism. It is important that, using the hollow cone illumination, the order selecting is also achieved simultaneously. Only the first order diffraction appears in the center circle defined by the hollow cone beam.

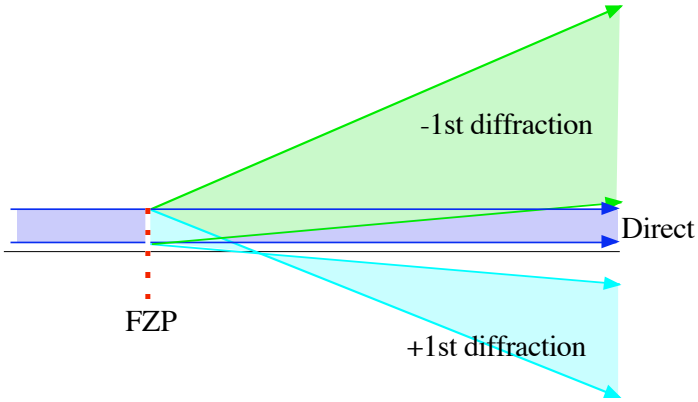

Fig. 3.1. Order-selecting for plane wave illumination. Only a half of FZP aperture is illuminated.

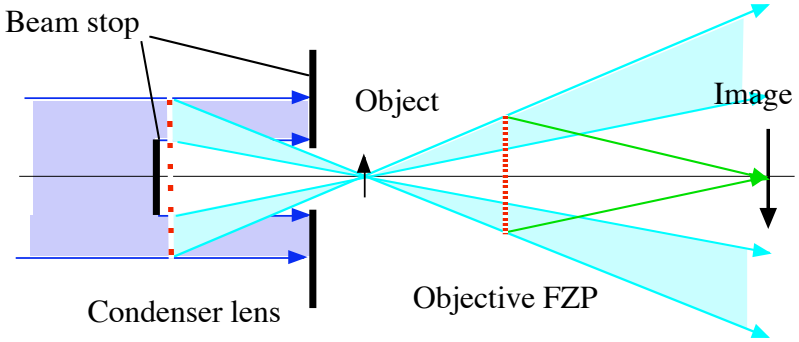

Fig. 3.2a Critical illumination with condenser zone plate and objective zone plate. Hollow cone illumination is used for diffraction order-selecting.

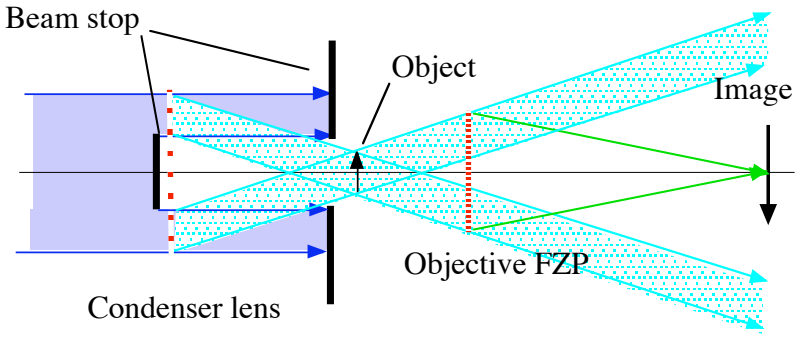

Fig. 3.2b Köhler's illumination with condenser zone plate. Hollow cone illumination is also achieved by combination with a center beam-stop and an aperture in front of object.

3.3. Spatial resolution of FZP microscopy with illuminating optics

Spatial resolution of imaging optics is essentially determined by the diffraction of light. That is the same as that of microfocusing optics. The diffraction-limited resolution for microscope with an objective

lens of circular aperture (axis-symmetric optics) and incoherent illumination (for example, self-emitting object) is expressed by the well-known Rayleigh's criterion as

$$\Delta = 0.61\ \lambda/NA, \qquad (3.1)$$

Where NA is so-called numerical aperture of objective lens defined as $NA = \sin\theta$. Here, the θ is the angle between marginal ray and optical axis, as shown in Fig. 3.3. It is also apparent from the diffraction of linear grating that the $\sin\theta$ is equal to the λ/d, where d is the outermost zone period of FZP. Then,

$$\Delta = 0.61d.$$

A formula of $\Delta = 1.22\ dr_N$ is frequently used, where dr_N is a half pitch of outermost zone period (or width of outermost zone). This is the same as that of micro-focusing optics.

Thus, the spatial resolution is, in principle, limited by the numerical aperture of objective lens, and the limitation is simply described by the diffraction theory as same as that of microbeam optics. However, when condenser lens optics is used, the spatial resolution is determined not only by the NA of objective but also by the convergent angle of illuminating beam. This is called matching of aperture. When the convergent angle is equivalent to the NA of objective lens, the spatial resolution is equal to that defined by the equation (3.1). The best resolution is achieved, when the NA of condenser is 1.5 times that of the objective lens. In this condition, the spatial resolution becomes ~$0.57\lambda/NA$. When the condenser optics is not used, i.e. in the case of plane wave illumination (coherent illumination), the spatial resolution is written as $0.82\lambda/NA$ instead of $0.61\lambda/NA$, as well.

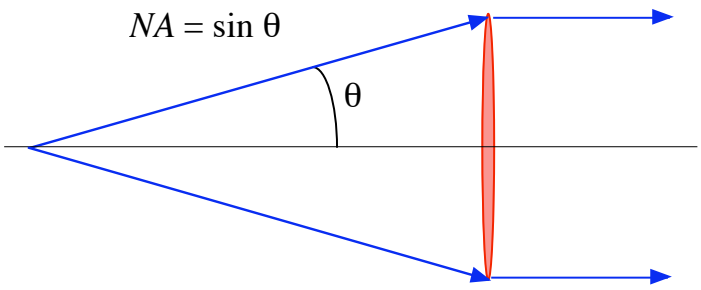

Fig. 3.3. Numerical aperture of objective lens.

3.4. Depth of focus

Hard x-ray microscopy has an advantage that thick samples can be observed in high spatial

resolution for its high tansmissivity and depth of focus. Although the depth of focus in hard x-ray microscope is generally much greater than that of optical microscope, the restriction by depth of focus is sometimes not negligible. The depth of focus can be evaluated by the geometrical optics, as shown in Fig. 3.4. When a point source is placed at a distance of D from the exact object plane, the image size extracted at the object plane is expressed as $2DNA$. The amount of defocusing, $2DNA$, should be less than or equal to the diffraction-limited resolution in order to neglect the influence to spatial resolution. By taking the both side of object plane into account, the depth of focus, $2D$, is expressed by

$$2D = 0.61\lambda/NA^2. \qquad (3.2)$$

Differently speaking, the NA of objective determines the ratio of field of view and spatial resolution. For an example, when λ = 1 Å, and $NA = 10^{-3}$, the diffraction-limited resolution is 61 nm, and the limit of sample thickness is 61 μm in diameter. It should be noted that the restriction on the depth of focus expressed by the equation (3.2) is essentially the same as the ultimate limitation on spatial resolution for finite sample thickness, $\Delta \sim (\lambda L)^{1/2}$, where L is thickness of sample.

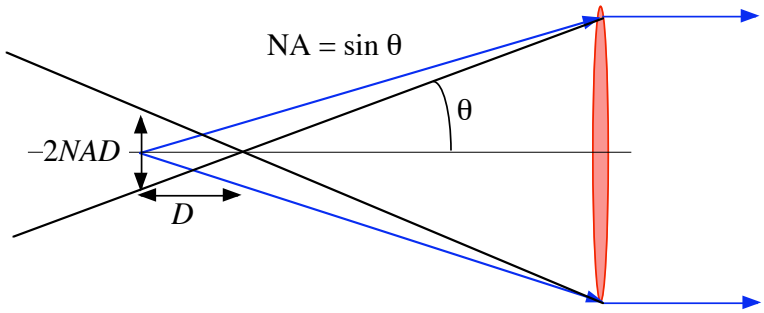

Fig. 3.4 Depth of focus. Black line represents primary focus, and blue line is marginal path of defocused rays.

3.5. Chromatic aberration and spherical aberration

In above discussion, perfectly monochromatic x-ray beam is assumed. However, real x-ray beam has some bandwidth, even if the crystal monochromator is used. The influence of the finite bandwidth of incident x-ray spectra is called chromatic aberration. The defocusing effect by the chromatic aberration is evaluated by the similar manner as that of depth of focus, as

$$\Delta f\, NA < 0.61\lambda/NA. \qquad (3.3)$$

Here, Δf is a displacement of focus caused by chromatic aberration. The focal length is defined by $r_n^2 = n\lambda f$. Here, the r_n is constant for given FZP, and the focal length, f, is proportional to $1/\lambda$. Then, the difference of focal length Δf is written as

$$\Delta f / f = \Delta\lambda/\lambda, \tag{3.4}$$

where $\Delta\lambda$ is bandwidth of incident radiation. Then, the equation (3.3) can be rewritten as

$$\Delta\lambda/\lambda\, f\, NA < 0.61\lambda/NA. \tag{3.5}$$

By using approximation of $NA \sim r_N/f$ and $r_N^2 = N\lambda f$, where N is the zone number of outermost zone, a useful formula is deduced as follows,

$$\Delta\lambda/\lambda < 0.61/N.$$

This formula gives a tolerance on bandwidth of incident x-ray beam for FZP microscope.

The spherical aberration comes from the approximation used to derive the equation (1.2). By using second higher order term, the equation is approximately rewritten as

$$r_n^2/2a - 1/8r_n^4/a^3 + r_n^2/2b - 1/8r_n^4/b^3 = n\lambda/2. \tag{3.6}$$

In the case of imaging microscope, $a << b$, and $a \sim f$. Then, the equation (3.6) can be written as

$$r_n^2/2a + r_n^2/2b - 1/8r_n^4/f^3 = n\lambda/2. \tag{3.7}$$

In order to evaluate the wave-front aberration, a Rayleigh's quarter wavelength criterion can be used. The $\lambda/4$ rule is that, when the optical path discrepancy from the primary path is within the quarter of wavelength, the influence of wave-front aberration to the spatial resolution may be ignored. Therefore, by comparing the equation (1.2) and equation (3.7), the $\lambda/4$ rule for the spherical aberration is expressed by

$$1/8r_N^4/f^3 < \lambda/4. \tag{3.8}$$

Using the fundamental structure of Fresnel zone plate, $r_N^2 = N\lambda f$, the relation is rewritten as

$$1/2N^2 < f / \lambda. \qquad (3.9)$$

This formula also gives a limitation on the number of outermost zone as well as the chromatic aberration. Although the spherical aberration can be perfectly erased by using the exact formula of equation (1.1), these zone plates can be used only at the fixed wavelength (λ) and fixed optical distances (a and b). These FZPs do not have flexibility. Therefore, FZPs defined by the conventional formula of equation (1.4) are much convenient for practical use.

3.6. Off-axis aberration theory based on wave optics

In this section, off-axis imaging property of FZP microscope is discussed. The optical path equation is written as

$$\{(r_a - r_n\cos\phi)^2 + (r_n\sin\phi)^2 + a^2\}^{1/2} + \{(r_b + r_n\cos\phi)^2 + (r_n\sin\phi)^2 + b^2\}^{1/2}$$
$$= n\lambda/2 + (a^2 + r_a^2)^{1/2} + (b^2 + r_b^2)^{1/2}, \qquad (3.10)$$

where $r_a/a = r_b/b$, as shown in the figure, and r_b/r_a (= b/a) represents the geometrical magnification of microscope. The ϕ is angle at a point of Fresnel zone plate objective as shown in Fig. 3.5. The influence to spatial resolution is evaluated by the similar manner as that on the spherical aberration. By using the second order approximation, the equation (3.10) is rewritten as

$$1/2(r_a^2 - 2\,r_a\,r_n\cos\phi + r_n^2)/a - 1/8(r_a^2 - 2\,r_a\,r_n\cos\phi + r_n^2)^2/a^3$$
$$+ 1/2(r_b^2 + 2\,r_b\,r_n\cos\phi + r_n^2)/b - 1/8(r_b^2 + 2\,r_b\,r_n\cos\phi + r_n^2)^2/b^3$$
$$= n\lambda/2 + 1/2(r_a^2/a) - 1/8(r_a^4/a^3) + 1/2(r_b^2/b) - 1/8(r_b^4/b^3). \qquad (3.11)$$

Then, the wavefront aberrations are analyzed by the optical path equation (3.11), and the Rayleigh's quarter wavelength rule is expressed as

$$|\{-\,r_a\,r_n\cos\phi/a + r_b\,r_n\cos\phi/b\} + 1/2\{\,r_n^2/a + r_n^2/b - n\lambda\}$$
$$-1/8\{(r_a^2 - 2\,r_a\,r_n\cos\phi + r_n^2)^2/a^3 - r_a^4/a^3 + (r_b^2 + 2\,r_b\,r_n\cos\phi + r_n^2)^2/b^3 - r_b^4/b^3\}|$$
$$< \lambda/4. \qquad (3.12)$$

The first term represents the magnification equation of $r_a/a = r_b/b$, and the second term corresponds to the basic zone plate equation of $r_n^2 = n\lambda f$. Then, the residual aberration is rewritten as

$$|1/8\{(-4\, r_a^3\, r_n \cos\phi/a^3 + 2\, r_a^2\, r_n^2/a^3 + (2\, r_a\, r_n\cos\phi)^2/a^3 - 4\, r_a\, r_n^3\cos\phi)/a^3 + r_n^4/a^3)$$
$$+ (4\, r_b^3\, r_n \cos\phi/b^3 + 2\, r_b^2\, r_n^2/b^3 + (2\, r_b\, r_n\cos\phi)^2/b^3 + 4\, r_b\, r_n^3\cos\phi)/b^3 + r_n^4/b^3)\}|$$
$$< \lambda/4. \qquad (3.13)$$

The aberration that includes first order of r_N can also be ignored, because the residual aberration is written as

$$|-1/8\{-4\, r_a^3\, r_N \cos\phi/a^3 + 4\, r_b^3\, r_N \cos\phi/b^3\}| < \lambda/4. \qquad (3.14)$$

This term is always zero, because $r_a/a = r_b/b$.

The residual off-axis aberration that consists of square of r_N is extracted from the (3.13) as

$$|1/8\{(2\, r_a\, r_N\cos\phi)^2/a^3 + 2\, r_a^2\, r_N^2/a^3 + (2\, r_b\, r_N\cos\phi)^2/b^3 + 2\, r_b^2\, r_N^2/b^3)| < \lambda/4. \quad (3.15)$$

By using $-1 \le \cos\phi \le +1$, and $a << b$ and $a \sim f$, the following expression is derived.

$$r_a^2 r_N^2/f^3 < \lambda/3. \qquad (3.16)$$

Concerning to the third order of r_N, following formula is extracted from the (3.13).

$$|1/8\{(-4\, r_a\, r_N^3\cos\phi)/a^3 + (4\, r_b\, r_N^3\cos\phi)/b^3\}| < \lambda/4. \qquad (3.17)$$

This expression may also be reduced as

$$r_a\, r_N^3/f^3 < \lambda/2. \qquad (3.18)$$

Concerning the fourth order term of r_N, the residual aberration is reduced as

$$|1/8(r_N^4/a^3 + r_N^4/b^3)| < \lambda/4. \qquad (3.19)$$

This formula is also approximated as

$$1/8r_N^4/f^3 < \lambda/4$$

This is the spherical aberration discussed in the previous section.

These formulas give a restriction on the maximum field of view for a given FZP to achieve a diffraction-limited resolution. By comparing (3.16) and (3.18) with the relation (3.2), it is apparent that the above conditions are generally well satisfied, when the field of view is less than the depth of focus. Therefore, from the point of view of three-dimensional observation, the Fresnel zone plate can be used as an objective lens for x-ray microscope without considering the off-axis aberrations, and the FZP imaging microscopy is applied to imaging microtomography in SPring-8

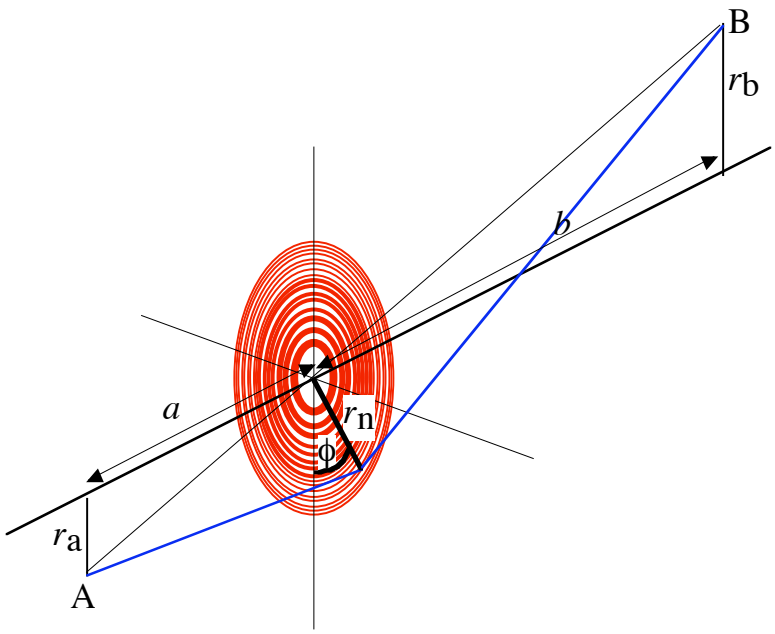

Fig. 3.5 Schematic diagram of off-axis optical path for FZP imaging optics.

3.7. Typical example of imaging microtomography with Fresnel zone plate objective in SPring-8

Typical experimental setup is schematically shown in Fig. 3.6. This microscopy/micro-tomography setup is installed at the beamline 47XU of the SPring-8. The light source is an in-vacuum planar undulator with permanent magnet array. The undulator radiation is monochromatized by liquid-nitrogen-cooling silicon 111 double crystal monochromator. The x-ray energy of 8 keV is selected in this experiment. The bandwidth of monochromatic x-ray beam through the crystal monochromator is

estimated be $\Delta\lambda/\lambda \sim 10^{-4}$. Therefore, the monochromaticity is sufficient for the zone plate objective.

Condenser optics is a specially designed zone plate with a constant grating pitch of 400 nm. The zone material is 1 μm-thick tantalum, and the diameter of zone plate is 500 μm. This condenser zone plate is used in combination with a center beam stop with a diameter of 300 μm in order to achieve hollow-cone illumination. The circle of least confusion is located at about 500 mm downstream of the condenser zone plate. Then, by placing the object at the circle of least confusion, a quasi-Köhler illumination condition is satisfied. In front of the object, a pinhole with a diameter of 100 μm was placed as an order-selecting-aperture for the condenser zone plate. The field of view is actually defined by this aperture. A beam diffuser made of charcoal powder (grain size of a few tens μm, and rotating at 600 rpm) is also placed upstream of the condenser zone plate for the purpose of reducing strong speckle noise due to high coherence of incident x-ray beam.

The objective zone plate is also made of tantalum with a thickness of 1 μm. The outermost zone width is 100 nm and the focal length is 100 mm at 8 keV. The diameter of object zone plate is 155 μm, and the number of zone is 388. Although the numerical aperture (convergent angle) of condenser optics is a half of that of objective lens, the influence to the spatial resolution is not serous in this case. An X-ray imaging detector is used to measure the three dimensional data at single scan. The imaging detector consists of a fine powder phosphor screen (P43, Gd2O2S:Tb), relay lens and cooled CCD camera (C4880-41S, Hamamatsu Phtotonis KK, Japan). A high-precision rotating stage made at Kohzu Precision Co. is used for sample rotation in tomographic measurement. The wobbling of rotation axis is measured to be ±70 nm within 360º rotation.

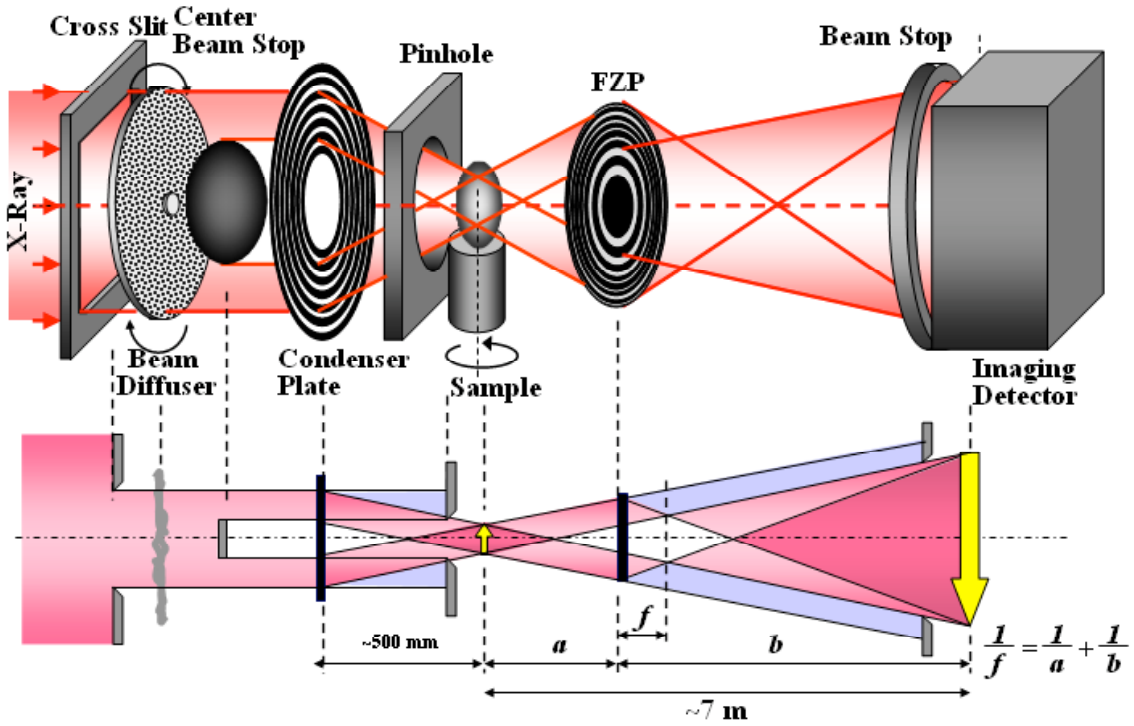

Fig. 3.6. Schematic diagram of experimental setup for imaging microtomography.

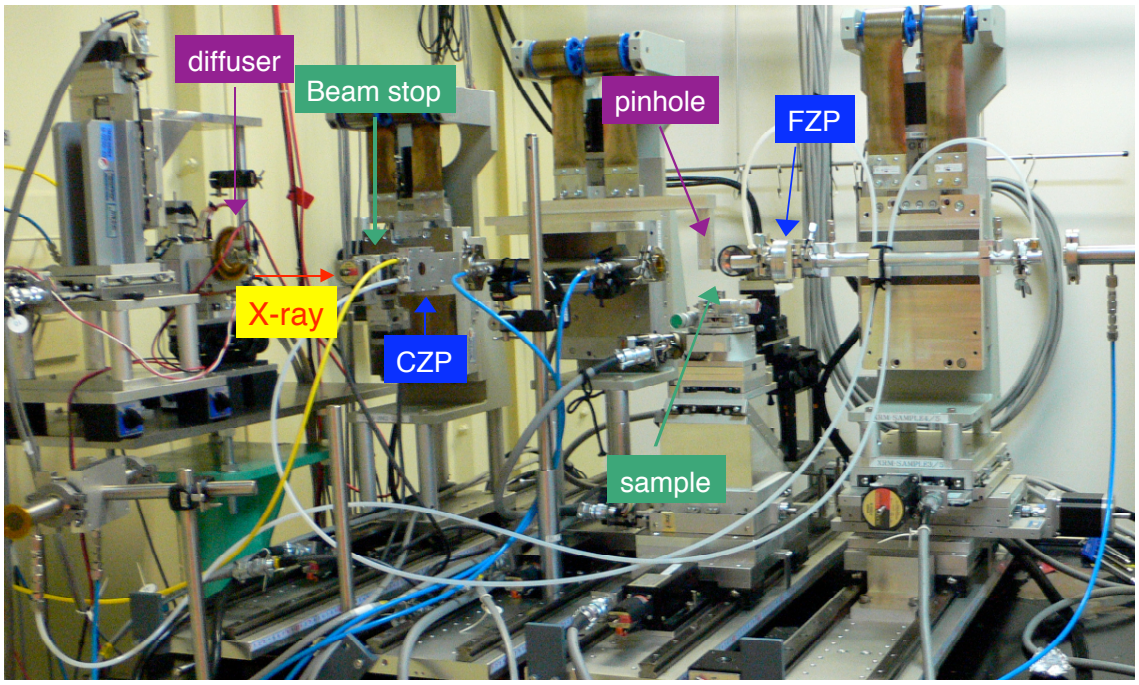

Fig. 3.7. Experimental setup. Condenser optics, sample stage and objective FZP are shown in the figure. The imaging detector is located 7 m from the objective FZP, right-hand side out of the figure.

Useful references for general understanding of optics

R. Feynman, R. Leighton and M. Sands: Lecture on Physics (Addison-Wesley),

M. Born and E. Wolf, Principles of Optics, (Cambridge University Press)

For specific topics on Fresnel zone plate optics (in soft x-ray regions),

D. Attwood, Soft X-rays and Extreme Ultraviolet Radiation, Principles and Applications (Cambridge University Press).

A. G. Michette, Optical Systems for Soft X-rays (Plenum Press).

Other references,

N. Kamijo, et al., Proc. of 8th Int. Conf. X-ray Microscopy, IPAP Conf. Series 7 (2006) 97-99.

B. Nieman, et al., AIP CP507 (2000) 440-405.

Y. Suzuki, et al., Jpn. J. Appl. Phys. 40 (2001) 1508-1510.

Y. Suzuki, et al., SPIE Proceedings 4499, (2001) 74-83.

Y. Suzuki, et al., Journal de Physique IV France 104 (2003) 35-40.

Y. Suzuki, Jpn. J. Appl. Phys. 43 (2004) 7311-7314.

Y. Suzuki, et al., Jpn. J. Appl. Phys. 44 (2005) 1994-1998.

Y. Suzuki and H. Toda, Advanced Tomographic Methods in Materials Research and Engineering, ed. John Banhart, Oxford University Press, (2008), Section 7.1 Fresnel zone plate microscopy and microtomography.

H. Takano, Y. Suzuki, and A. Takeuchi, Jpn. J. Appl. Phys. 43 (2003) L132-L134.

A. Takeuchi, et al., Jpn. J. Appl. Phys. 40 (2001) 1499-1503.

A. Takeuchi, Y. Suzuki, and H. Takano, J. Synchrotron Radiation 9 (2002) 115-118.

A. Takeuchi, et al., Rev. Sci. Instrum. 73 (2002) 4246-4249.

S. Tamura, et al., J. Synchrotron Rad. (2002) 9, 154-159.

K. Uesugi, A. Takeuchi, and Y. Suzuki, (2006), Proc. of SPIE 6318, 63181F.

D. Weiß, et al., Ultramicroscopy 84 (2000) 185-197.

Basic exercises, before the experiment

1. Calculating the radius of some rings of the FZP in Fig. 1.2, and total number of zone.

2. Calculate the focal length of the FZP in Fig. 1.2 for 8 keV x-rays.

3. Calculate the exact focal point for a given source to FZP distance (depending on the beamline optics).

--> For example, source to FZP distance is 46 m (BL47XU)

4. Calculate the geometrical spot size, assuming a beamline where you will do the microfocusing experiment.

--> Source size of SPring-8 is ~ 40 μm vertically and ~ 600 μm horizontally.

5. The monochromaticity of x-ray beam is sufficient for the FZP in Fig. 1.2 at your beamline (with a conventional crystal monochromator)?

--> Look at the optics of beamline from WEB or ask to beamline staff.

6. Calculate the depth of focus for the FZP shown in Fig. 1.2.

7. How is the optimized thickness of zone for 8 keV x-rays? Assume the zone material of gold or tantalum.

8. Drawing the sinc function and Laue function for a given slit and grating.

--> 10 μm slit, 1 Å wavelength, and 100 line grating.

9. Introducing a relation between required monochromaticity ($\lambda/\Delta\lambda$) and number of zone (N), using the Laue function for N-period grating.

10. Which kind of pin-hole should be used as the order-selecting-aperture? Diameter, material and thickness, considering work distance of optics.

--> Once, use 0.5 center stop disc.

11. Calculate the zone plate parameter of the FZP in Fig. 1.2 with a center stop of 50 μm-diameter.

Practice at the beamlines – microfocus beam

1. General understanding on the beamline optics.

Configuration of beamline 20XU is shown below as an example.

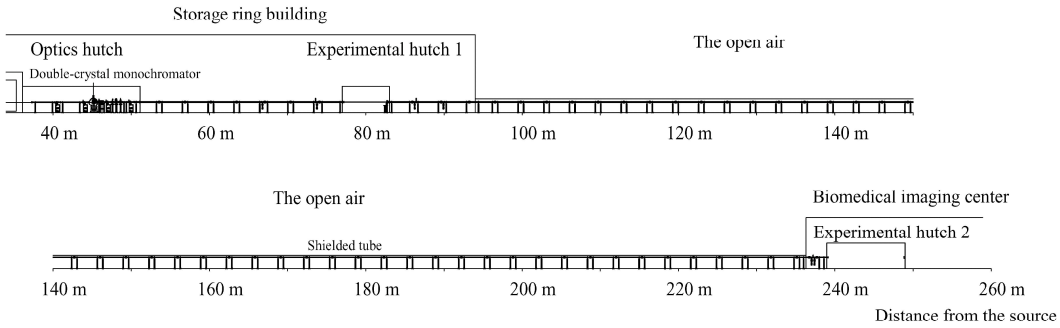

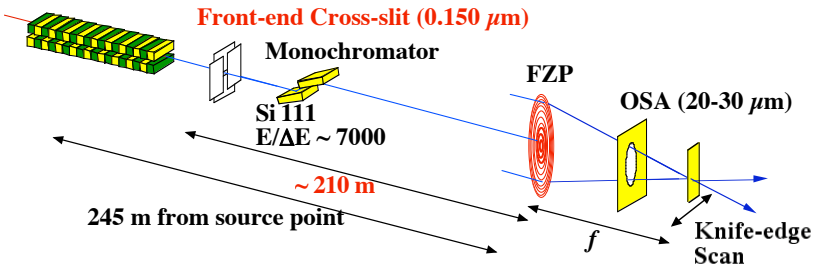

Experimental Setup of Micro-focusing at BL20XU

2. Finding FZP and order-selecting-aperture, using x-ray imaging detectors.

3. Alignment of FZP and OSA on optical axis.

4. Searching for the fundamental (first-order) diffraction.

5. Finding the focal point by means of Foucault's knife-edge test.

Far-field image varies as shown below.

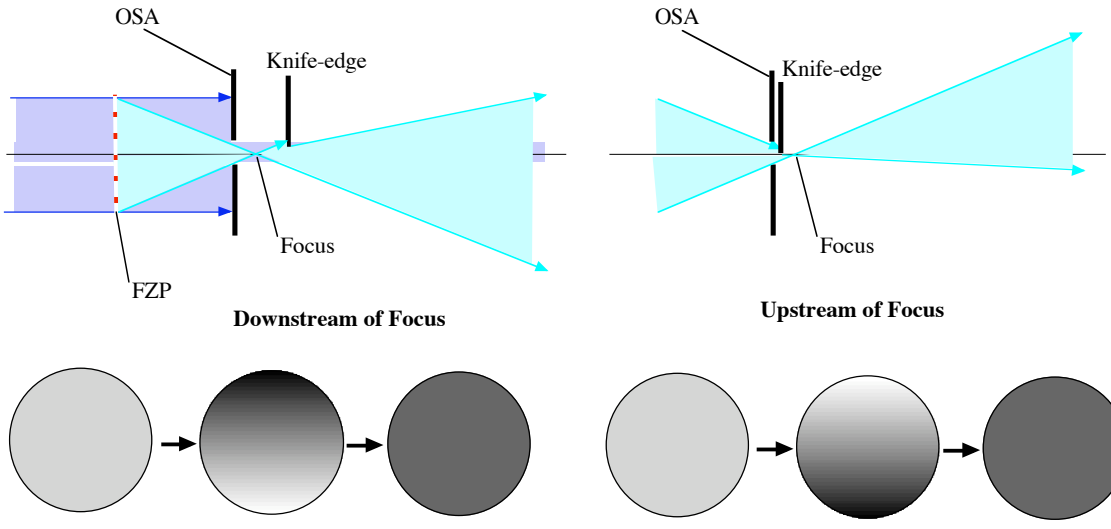

6. Measurement of beam size by differential knife-edge scanning method, and comparison to theoretical value.

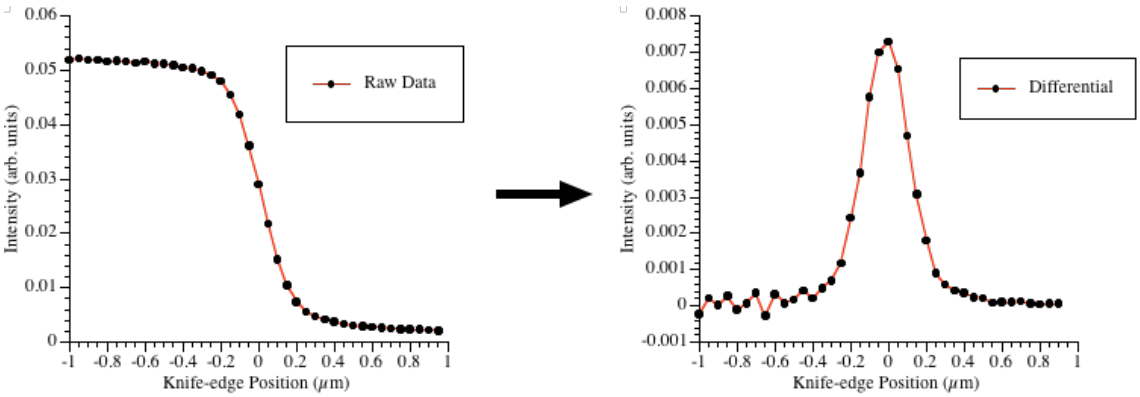

7. Changing the front-end slit size, dependence of focus beam size on spatial coherence condition.

8. Only at BL47XU, measurement of stigmatism for light source, and elimination of the stigmatism by anti-bending of pre-mirror.

Practice at beamline – imaging microscopy with parallel beam illumination

1. Setting the instruments

Spatial filter in front of sample, FZP, and imaging detector,

2. Searching for the FZP. Observing the diffraction from FZP, and separating the positive, negative and direct beams by the spatial filter**.**

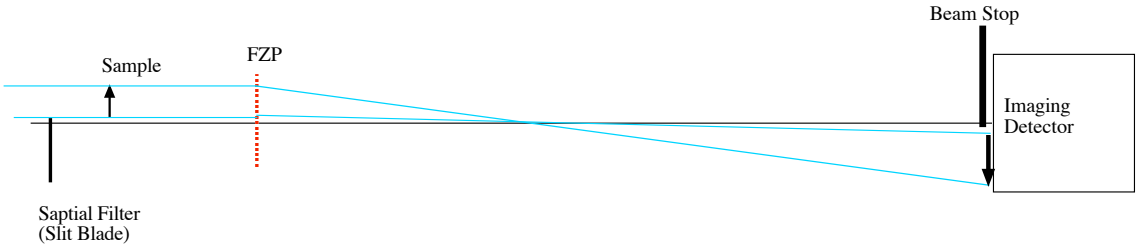

3. Put a He path between FZP and imaging detector, and setting a direct beam stop in front of the imaging detector.

4. Observing some test objects, and how we can adjust the focus?

5. Imaging properties. Change the beam coherence by using a diffuser in front of object.

Advanced exercises,

1. Calculate the diffraction efficiency, and comparison to the experimental result.

2. Calculating and experimentally testing of chromatic aberrations, how is the tolerance of wavelength and bandwidth?

3. Theoretical estimation and experimental test of the depth of focus by changing the position of knife-edge.

4. Influence of mask in front of FZP, shading half of FZP aperture. Both vertical and horizontal focusing properties. This experiment must be done for the diffraction-limited resolution case.

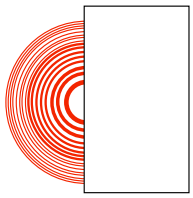

5. Influence of mask in front of FZP, center obstacle. This experiment also requires diffraction-limited resolution.

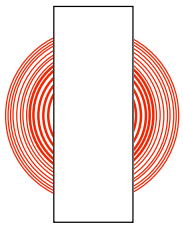

6. Inserting something in the optical path, how is the disturbance of wave-front, for instance, putting a sheet of paper, Kapton foil, aluminum foils, etc?

7. Inclination of FZP and focusing properties, how is the tolerance for angular misalignment?

8. Focusing properties of higher order diffractions, how is the diffraction-limited resolution, and diffraction efficiencies?

9. The longitudinal source size of SPring-8 undulator is 4.5 m. This length of light source gives some problem on focusing properties?

10. Focusing properties for off-axis undulator radiation. How is the effective angular size of undulator radiation? and its relation to inclination to optical axis (electron orbit). This experiment should be done at the short beamlines. The BL47XU is preferable.

11. At the undulator beamlines, the x-ray source is very long. SPring-8 standard undulator has a longitudinal length of 4.5 m. When a demagnified image of source is generated by an optical lens, the front end and the rear end of undulator, for example, may yield different foci. It is actually problem?